Filter Wheel Design for Optimal Color Reconstruction

K D Fram[1], R K Mantiuk[1] and G D Finlayson[2]

[1]Computer Science, University of Cambridge, Cambridge, UK
[2]Computing Sciences, University of East Anglia, Norwich, UK

E-mail: kdf25@cam.ac.uk

Abstract.
Spectral sensitivity functions of cameras with a fixed set of color filters often result in color measurements that do not match those captured by the human eye. This can lead to inaccurate color reproduction in images, especially under certain lighting conditions. One solution to this problem is to use a filter wheel with a set of filters that can be combined to reconstruct specific color matching functions. We design a framework for selecting filters from a given set to optimize for accurate color reconstruction, and apply this framework to the Rosco Supergel filter set. We also generalize our framework for other color matching functions beyond the CIE 1931 XYZ CMFs.

1 Introduction

Multispectral image acquisition systems have uses ranging from agricultural monitoring to fine art analysis to medical scanning [1, 2, 3, 4, 5, 6, 7, 8]. State of the art systems are prohibitively costly [9], and are generally only suitable for their specialized purpose. A comparatively cheaper and more flexible solution lies in the filter wheel, notably employed in terrestrial and geological analysis as early as 1972 [10], and now provides a useful framework for multispectral imaging. In this paper, we construct an effective system using simple 3D-printed components, microcontrollers such as the Raspberry Pi, and a set of inexpensive gel filters such as those used for stage lights.

However, our aim is to improve upon the classic apriori fixed filter wheel used with a monochromatic camera. Here, we simulate image capture through a set of colored filters and then combine these to best approximate the desired XYZ colorimetric values, effectively solving for a new color wheel.

Prior work has been limited by computational resources, and generally relies on heuristic measures to select filters [11, 12]. We provide a minimal error reconstruction for the set of Rosco Supergel [13] filters.

Further, we provide a framework for filter selection for any target spectral response function. By generalizing our target function, we allow for applications beyond RGB reconstruction, such as hyperspectral and multispectral imaging. Additionally, we explore the performance of our system under different human eye color matching functions, such as CIE 1931 [14] and CIE 2006 XYZ (from LMS) functions [15]. In the analysis of human eye color matching functions, we approach Luther Condition Compliance, which is the condition that a camera's spectral sensitivity functions are a linear transformation of the human eye's color matching functions [16].

Finally, we show that our methodology provides accurate reconstruction by evaluating the 24 Macbeth Color Checker patches and computing ΔE_{2000} under standard illuminant for the CIE 2006 XYZ target functions prescribed from CVRL [15]. We compute the relationship between number of filters k and minimum

ΔE_{2000}.

2 Related Work

2.1 Filter Wheel Design

The spinning filter wheel construct provides an inexpensive solution when unconstrained by capture duration, such as in the imaging of fine art and in agricultural applications. Morales et al. [17] demonstrate a bandpass filter wheel utilized for precision agriculture applications, and Scutelnic et al. [9] propose a similar filter wheel construct to build a relatively low cost sensor array. Lapray et al. [18] provide an overview of multispectral imaging technologies as well as their costs, providing a benchmark for our work.

2.2 Image Response

Much of the existing literature on simulation of color matching functions relates to the CIE XYZ models of the human eye. We follow the work of Gao et al. [19] in matching our simulated camera's spectral sensitivity function to the human eye by optimizing for a color correction matrix $\boldsymbol{M}$ best matching the set of filtered camera sensitivities to the XYZ color matching functions. This method achieves optimality only when we approach Luther Condition compliant capture [20], specifically that our spectral sensitivity functions be linearly related to our chosen XYZ color matching function. We follow the work of Finlayson and Zhu [21] in their analysis of Luther-condition compliant filters. However, rather than designing a specialized filter, we investigate whether we can approach Luther compliance by adding incrementally more generic filters to our filter wheel.

In our model, we have a single grey-scale camera (only a brightness channel). Thus, our estimated new camera sensitivities are a function of the intrinsic sensitivities of this single-channel camera multiplied by the filter transmittance. Let $f_i(\lambda)$ respectively denote the i'th filter's spectral transmission function, and let $m_{c,i}$ denote the transformation weights for combining the i'th filter into color channel c (e.g. to best approximate the XYZ color matching functions).

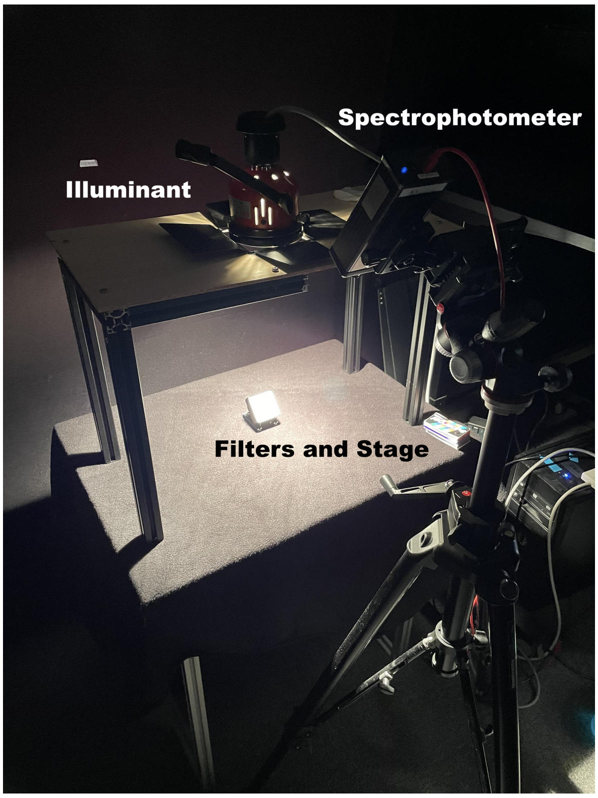

Figure 1: Filter measurement setup with spectrophotometer and Rosco Supergel filters.

Then the effective spectral camera sensitivity function θ_c can be written as:

$$\theta_c(\lambda) = \sum_{i \in I} m_{c,i} f_i(\lambda) \sigma(\lambda) \quad (1)$$

where I denotes the set of k indices from our set of N filters and $\sigma(\lambda)$ denotes the sensor's spectral sensitivity function.

In the optimizations that follow, we will solve for the R, G and B sensors that best approximate the actual X, Y and Z color matching function sensitivities, respectively referred to as $x_c \in \{X, Y, Z\}$.

3 Method

3.1 Data Collection

The aim of our method is to capture multiple images through different color filters and then combine them to match the colors of an image of a scene captured with respect to the CIE XYZ color matching functions (CMFs). We will choose filters drawn from a set of Rosco Supergel filters that we measure in our lab. We model our camera's and optional IR-cut filter's spectral response function as per the manufacturer's specifications [22, 23] All filters are represented in the domain $\omega = [400, 750]$ nm.

3.2 Problem Formulation

For approximations of XYZ, we follow the work of Hardeberg [11] in adopting MSE loss between target and simulation over the visible spectrum as the loss function and minimizing loss via search for an optimal $\boldsymbol{M}$, the $3 \times k$ matrix of $m_{c,i}$ transformation weights. For each color channel c we have MSE loss L_c as:

$$L_c = \int_{\omega} \|x_c(\lambda) - \theta_c(\lambda)\|_2 d\lambda \qquad (2)$$

Given that we are limited by 1 nanometer steps in measurement, we discretize over ω, taking $\omega_d = \{400, 401...750\}$, and functions having arguments in brackets representing functions, for example $\theta_c[\lambda]$, evaluated over discrete domain. We take MSE loss over ω_d to compute our total loss per color channel:

$$L_c = \frac{1}{|\omega_d|} \sum_{\lambda \in \omega_d} \|x_c[\lambda] - \theta_c[\lambda]\|_2 \qquad (3)$$

We consider loss from all color channels equally, and minimize $\sum_c L_c$ by choosing $\boldsymbol{M}$ for a set of I 'active' filters, each having transmission functions $f_i[\lambda]$ over ω_d, thus comprising a k length vector of functions. Omitting the constant $\frac{1}{|\omega_d|}$, we have for each set of filters I:

$$\arg\min_{\mathbf{M}} \sum_{c} \sum_{\lambda \in \omega_d} \|x_c[\lambda] - \sum_{i \in I} m_{c,i} f_i[\lambda] \sigma[\lambda]\|_2 \qquad (4)$$

We define $\boldsymbol{F}$ as the stacked and discretized $k \times 351$ matrix of $f_i[\lambda]\sigma[\lambda]$ measured at each $\lambda \in \omega_d$. And the discretized set of 3×351 XYZ functions as $\mathbf{X}$.

When using a least-squares loss L_d, we can solve for $\boldsymbol{M}$, in closed form, using the Moore-Penrose pseudo-inverse [24, 25], denoted A^+ for a matrix A. The unique $351 \times k$ Moore-Penrose pseudo-inverse solution $\boldsymbol{F}^+$ has the desirable property that while we may not exactly satisfy the Luther condition, it provides the closest possible approximation for a given set of filter indices I [26]:

$$\boldsymbol{M} \approx \boldsymbol{X}\boldsymbol{F}^+ \qquad (5)$$

Finally, as a point of detail we must alter this optimization if any of our filters have 0 transmission in a part of the assumed wavelength interval. The IR-cut filter only has nonzero transmittance in [400,650] nanometers. So, when this filter is used we can only optimize within this wavelength interval, and thus we redefine $\omega_d = \{400, 401, ...650\}$.

3.3 Filter Selection

While the number of filters N may be large, we ideally would posit a filter wheel with fewer filters.

3.3.1 Brute Force Search In the naive solution, we find the optimal filter combination for every subset of k filters (where k is small) drawn from the N filter set by selecting the combination with the lowest loss, considering all combinations of 119 Rosco Supergel filters (there are nearly 200,000,000 of these for $k = 5$). In Figure 2 we plot the errors across all sets of 5 filters (multiplied by the camera sensitivity) from the worst to best performing quintuple. We compute the Moore-Penrose pseudo-inverse for each set of filters. Our implementation is parallelized over 8 NVIDIA L4 GPUs, with a combined pool of up to 192GB VRAM, enabling us to compute brute force searches of $k = 5$ in approximately 7 minutes.

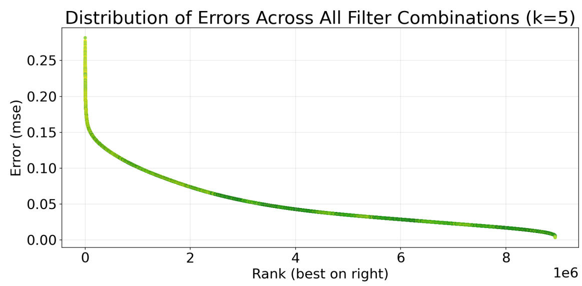

Figure 2: MSE Error distribution across all filter combinations for k=5

3.3.2 PCA Analysis To find the optimal filter combination without brute force search, we can use PCA analysis to find approximate solutions.

This method initially creates one $3 \times M$ matrix $\boldsymbol{M}$ and iteratively selects until reaching k filters and thus our final $3 \times k$ matrix of weights. Specifically, the selection is performed by projecting $\boldsymbol{F}$ onto the space spanned by the target $\boldsymbol{X}$ matrix, finding the filter with the highest norm as per the Matching Pursuit method outlined in Mallat and Zhang [27]. We iteratively apply this methodology k times, each time on a subset of the resultant orthonormal basis formed by subtracting the selected filter's projection.

This method is comparatively fast, able to compute the $k = 5$ case in 19 seconds on a single L4 GPU. This method also scales well, with $k = 8$ runtime at only 20 seconds.

We show the relative timings for Brute Force and PCA algorithms below.

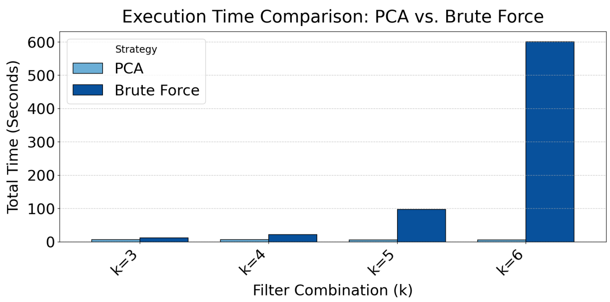

Figure 3: Execution Time Comparison between PCA and Brute Force Selection Methods

However, we note the improved MSE result for the brute force selection methodology.

3.3.3 Brute Force Search Augmented PCA While brute force methods guarantee minimum possible error by investigating the entire search space, large k implementations render this technique impractical. Additionally, our PCA method outlined above cannot always identify the optimal filter set, and has a non-negligible MSE shortfall vs. exhaustive search for all $k > 1$.

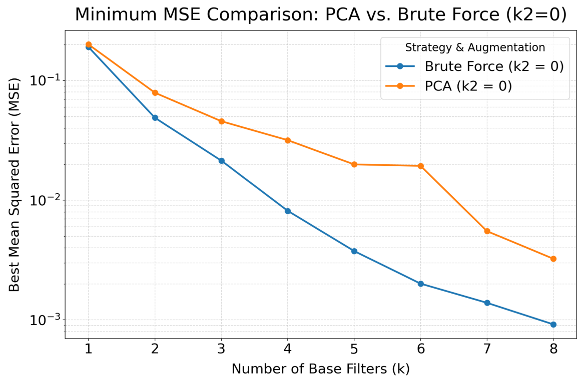

Figure 4: MSE Comparison between PCA and Brute Force Selection Methods, $k_2 = 0$

To address this problem, we use a blended method which finds a PCA solution for k_1 filters, and then considers all further possible combinations from a further k_2 filters, for a total $k = k_1 + k_2$. This provides a middle ground to the performance-accuracy tradeoff. There is negligible MSE difference between brute force and PCA methods at $k_2 > 1$ for all k_1. Further, for $k_2 < 4$, the added time from the exhaustive search step is between 5-20 seconds on the 8 aforementioned L4 GPUs.

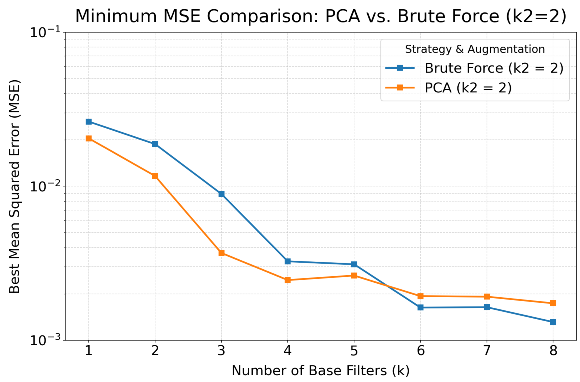

Figure 5: MSE Comparison between PCA and Brute Force Selection Methods, $k_2 = 2$

4 Evaluation

We evaluate our method by comparing the reconstructed XYZ color matching functions from our selected filters to the target XYZ functions, summarized by the MSE loss. We also consider the color difference ΔE_{2000} for a set of reflectances. This latter method effectively approximates the human eye's response to color difference, and is therefore well suited for a practical evaluation of our reconstruction [28]. For the latter evaluation, we use the Macbeth Color Checker [29] as our test set, and render XYZs and our RGBs (found from our method to best approximate XYZs) under a D65 illuminant.

In Figure 6, we show the best ΔE_{2000} of our approximation at each k filter subset of the Rosco Supergel set, where $k \in [1, 8]$. For completeness, we use brute force search.

In our evaluation, we utilize the python `color` and `colour-science` libraries, with the the CIE 1931 or 2015 2 Degree Standard Observer respectively, depending on whether we utilize the CIE 1931 or CIE 2006 XYZ functions. D65 illuminant from the same library is used as well as ColorChecker N Ohta reflectance patches. XYZ responses were converted to CIELAB using the `color.xyz2lab` function to convert XYZ signals to lab before ΔE_{2000} computation.

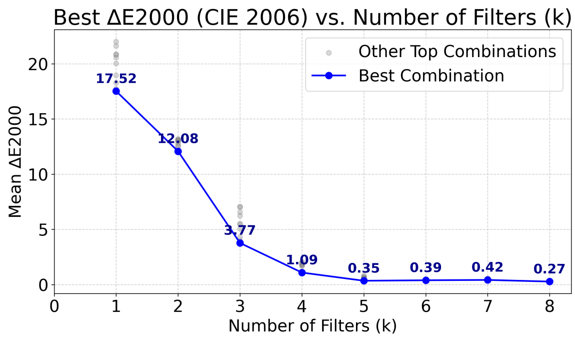

Figure 6: Best ΔE_{2000} for each number of filters k

We also plot the resultant reconstructed XYZ functions for the best $k-$filter combination of $k \in \{3, 4, 5, 6\}$, see respectively Figures 7, 9, 10 and 12.

Figure 7: Camera Spectral Sensitivity for best XYZ Reconstruction for $k = 3$

The best filter combination for $k = 3$, clearly a poor spectral fit, see Fig. 7, achieves a tolerable mean ΔE_{2000} of 3.77. This is in the just noticeable difference threshold of 2-4 [30], indicating that the reconstructed colors may be distinguishable from the target colors under certain conditions. The 24 patches below show the original in the top left of each pane and the simulated reconstruction in the bottom right, both rendered after transformation from XYZ to sRGB. For $k = 3$, it is evident there is a visible color difference.

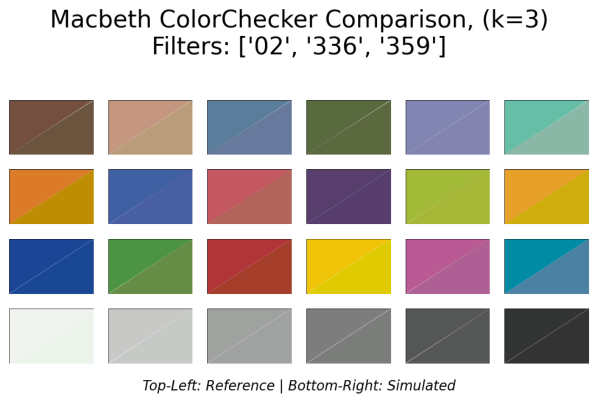

Figure 8: Macbeth Color Checker Comparison for $k = 3$

We see a noticeable improvement in MSE and in ΔE_{2000} with $k = 4$, the latter measuring 1.09, slightly above the 'just noticeable difference' of 1.0 [30].

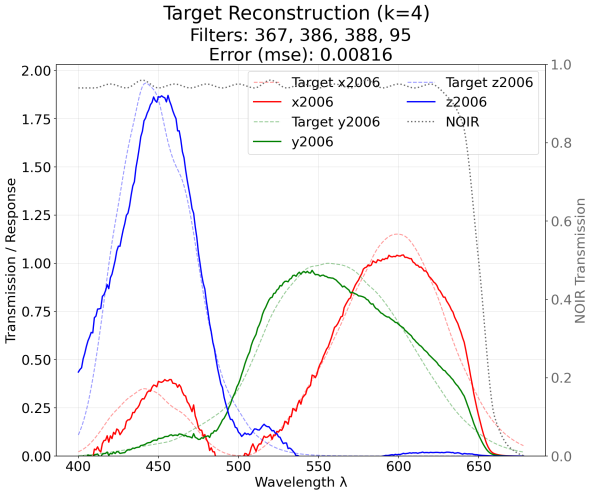

Figure 9: Camera Spectral Sensitivity for best XYZ Reconstruction for $k = 4$

Next, $k = 5$ achieves a ΔE_{2000} of 0.35, which is well below the just noticeable difference threshold, indicating that the reconstructed colors are likely indistinguishable from the target colors under typical viewing conditions.

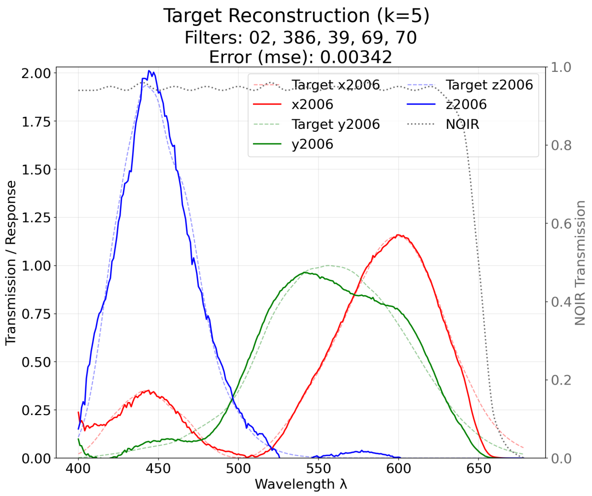

Figure 10: Camera Spectral Sensitivity for best XYZ Reconstruction for $k = 5$

The following Macbeth color patches display nearly identical hues between target and simulated patches.

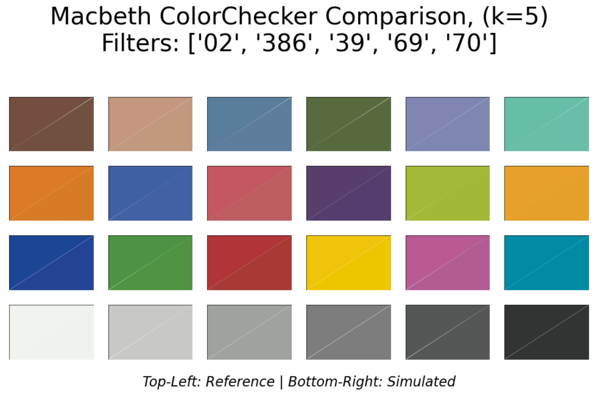

Figure 11: Macbeth Color Checker Comparison for $k = 5$

Finally, $k = 6$ achieves a ΔE_{2000} of 0.39, and there is generally limited further decrease in ΔE_{2000} at $k > 6$. Notice here the spectral fit of the XYZ CMFs is good.

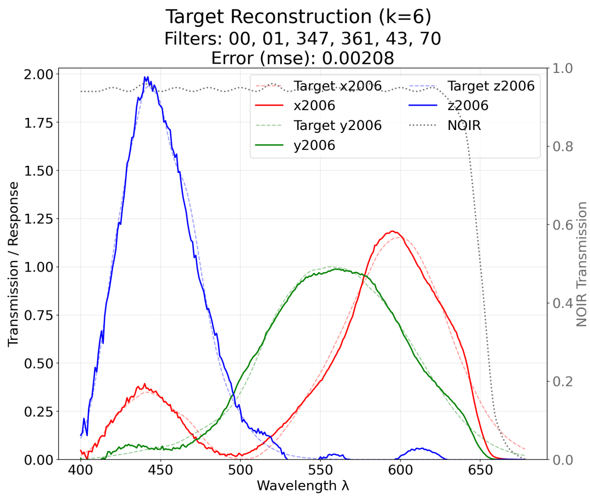

Figure 12: Camera Spectral Sensitivity for best XYZ Reconstruction for $k = 6$

5 Conclusion

We are able to achieve fairly accurate reconstructions of the XYZ color matching functions with as few as $k = 4$ filters, and very high quality reconstructions with $k > 5$ filters. This suggests that a filter wheel system with 6 filters could be sufficient for high-quality color reconstruction. However, the system does have drawbacks, such as shutter speed on the order of seconds and the need for a static scene.

References

[1] S. Peyghambari and Y. Zhang, "Hyperspectral remote sensing in lithological mapping, mineral exploration, and environmental geology: an updated review," *Journal of Applied Remote Sensing*, 2021.

[2] S. Ortega, H. Fabelo, D. K. Iakovidis, A. Koulaouzidis, and G. M. Callico, "Use of hyperspectral/multispectral imaging in gastroenterology. shedding some-different-light into the dark," *Journal of Clinical Medicine*, vol. 8, no. 1, p. 36, 2019.

[3] K. d. C. Mariotti, R. S. Ortiz, and M. F. Ferrão, "Hyperspectral imaging in forensic science: An overview of major application areas," *Science & Justice*, vol. 63, pp. 387–395, 2023.

[4] J. Qin, K. Chao, M. S. Kim, R. Lu, and T. F. Burks, "Hyperspectral and multispectral imaging for evaluating food safety and quality," *Journal of Food Engineering*, vol. 118, pp. 157–171, 2013.

[5] D. Wu and D.-W. Sun, "Advanced applications of hyperspectral imaging technology for food quality and safety analysis and assessment: A review - part i: Fundamentals," *Innovative Food Science and Emerging Technologies*, vol. 19, pp. 1–14, 2013.

[6] K. R. Lee, A. J. Richardson, E. Walowit, M. A. Crognale, and M. A. Webster, "Predicting color matches from luminance matches," *Journal of the Optical Society of America A (JOSA A)*, vol. 37, no. 4, pp. A35–A43, 2020.

[7] I.-C. Wu, Y.-C. Chen, R. Karmakar, A. Mukundan, G. Gabriel, C.-C. Wang, and H.-C. Wang, "Advancements in hyperspectral imaging and computer-aided diagnostic methods for the enhanced detection and diagnosis of head and neck cancer," *Biomedicines*, vol. 12, p. 2315, 2024.

[8] B. Lu, P. D. Dao, J. Liu, Y. He, and J. Shang, "Recent advances of hyperspectral imaging technology and applications in agriculture," *Remote Sensing*, 2020.

[9] D. Scutelnic, R. Muradore, and C. Daffara, "A multispectral camera in the vis–nir equipped with thermal imaging and environmental sensors for non invasive analysis in precision agriculture," *HardwareX*, vol. 20, p. e00596, 2024.

[10] H. Mannheimer, "The LANDSAT program," in *Proceedings of the Conference on Waste Heat Management and Utilization*, vol. 2, NASA, 1977.

[11] J. Y. Hardeberg, "Filter selection for multispectral color image acquisition," pp. 105–110, 03 2004.

[12] M. J. Vrhel and H. J. Trussell, "Filter considerations in color correction," *IEEE Transactions on image processing*, vol. 3, no. 2, pp. 147–161, 1994.

[13] Rosco Laboratories, "Rosco mycolor." `https://legacy.rosco.com/mycolor/mycolor.cfm`, 2026. Accessed: 2026-03-29.

[14] T. Smith and J. Guild, "The C.I.E. colorimetric standards and their use," *Transactions of the Optical Society*, vol. 33, pp. 73–134, Jan. 1931.

[15] A. Stockman and L. T. Sharpe, "Colour & vision research laboratory (cvrl)." `http://www.cvrl.org/`, n.d. Accessed: 2025-05-11.

[16] R. Von Luther, “Aus dem gebiet der farbreizmetrik,” *Zeitschrift fur Technishe Physik*, vol. 12, pp. 540–558, 1927.

[17] A. Morales, R. Guerra, P. Horstrand, M. Diaz, A. Jimenez, J. Melian, S. Lopez, and J. F. Lopez, “A multispectral camera development: From the prototype assembly until its use in a uav system,” *Sensors*, vol. 20, no. 21, p. 6129, 2020.

[18] P.-J. Lapray, X. Wang, J.-B. Thomas, and P. Gouton, “Multispectral filter arrays: Recent advances and practical implementation,” *Sensors*, vol. 14, no. 11, pp. 21626–21659, 2014.

[19] H. Gao, R. K. Mantiuk, and G. D. Finlayson, “Color-accurate camera capture with multispectral illumination and multiple exposures,” in *Computer Graphics Forum*, vol. 43, p. e15252, Wiley Online Library, 2024.

[20] H. E. Ives, “The transformation of color-mixture equations from one system to another,” *Journal of the Franklin Institute*, vol. 180, no. 6, pp. 673–701, 1915.

[21] G. D. Finlayson and Y. Zhu, “Designing color filters that make cameras more colorimetric,” *IEEE Transactions on Image Processing*, vol. 30, pp. 853–867, 2020.

[22] Arducam, “1mp ov9281/ov9282 global shutter camera,” n.d. Accessed: 2026-04-13.

[23] Coligh, “Shortpass filter ir cut 650nm,” n.d. Accessed: 2026-04-13.

[24] T. N. Greville, “Some applications of the pseudoinverse of a matrix,” *SIAM review*, vol. 2, no. 1, pp. 15–22, 1960.

[25] F. J. Beutler, “The operator theory of the pseudo-inverse i. bounded operators,” *Journal of Mathematical Analysis and Applications*, vol. 10, no. 3, pp. 451–470, 1965.

[26] R. MacAusland, “The moore-penrose inverse and least squares,” *Math 420: Advanced Topics in Linear Algebra*, vol. 551, pp. 1–10, 2014.

[27] S. G. Mallat and Z. Zhang, “Matching pursuits with time-frequency dictionaries,” *IEEE Transactions on signal processing*, vol. 41, no. 12, pp. 3397–3415, 1993.

[28] S. P. Farnand, “Using [delta] e metrics for measuring color difference in hard copy pictorial images,” in *Color Imaging VIII: Processing, Hardcopy, and Applications*, vol. 5008, pp. 109–118, SPIE, 2003.

[29] D. Pascale, “Rgb coordinates of the macbeth colorchecker,” 2006.

[30] P. Lindström, “Delta e blues: The science of color perception.,” *Seybold Report: Analyzing Publishing Technologies*, vol. 8, no. 3, 2008.